

Microstructure and Phase Transformation Behavior of a Stress-Assisted Heat-Treated Ti-Rich NiTi Shape Memory Alloy

A. Ahadi and E. Rezaei

(Submitted April 5, 2011; in revised form September 29, 2011)

In this study, the effects of stress-assisted heat treatment on the microstructure and phase transformation of a Ti-rich (Ti-49.52 at.% Ni) shape memory alloy were investigated. For this purpose, the alloy was heat treated at temperature of 500 °C for 10 h under applied stresses of 100 and 200 MPa. XRD, TEM, and repeated thermal cycling were employed to study the microstructure and transformation behavior of the heat-treated materials. Room temperature XRD diffractogram of the stress-free heat-treated material showed a weak reflection of austenite (B2), while that for the stress-assisted heat-treated materials had a high intensity implying the presence of residual austenite in the microstructure. TEM observations confirmed the presence of residual austenite and revealed mechanical twins as another constituent of the microstructure in the stress-assisted heat-treated materials. Moreover, with increasing the value of applied stress the size of mechanical twins was increased and a high density of structural defects was observed at the interfaces of the twins. DSC results demonstrated two-stage transformation in the initial cycles of transformation in the stress-assisted heat-treated material. After about eight cycles of transformation, the two-stage transformation has vanished, and a single-stage transformation remained up to 100 cycles. It was suggested that the accommodation of stresses at Ti₂Ni/matrix interface provides a suitable condition for local transformation of B2 to B19' that is manifested by a two-stage phase transformation. Introduction of structural defects during repeated thermal cycling may counteract the stress field at Ti₂Ni/matrix interface leading to a single-stage transformation.

Keywords mechanical twins, stress accommodation, stress-assisted heat treatment, two-stage phase transformation

1. Introduction

During the past few decades, NiTi shape memory materials have been exploited for myriad medical and industrial applications (Ref 1, 2). A thermoplastic martensitic transformation is responsible for the interesting properties observed in shape memory materials such as shape memory and Two-way shape memory effect. In order to modify the martensitic phase transformation, different approaches have been employed with respect to the alloy system. In near equi-atomic alloys, owing to lack of precipitates, thermomechanical processing is used for modification of phase transformation (Ref 3). Since precipitation is prevalent in Ni-rich alloys, aging is commonly used to modify transformation (Ref 4, 5). The stress field around fine and coherent Ni-rich precipitates is very effective in modification of martensitic transformation. However, in Ti-rich alloys, aging is less effective in alteration of transformation (Ref 6) due to

vertical solubility in NiTi phase diagram at Ti-rich side (Ref 7). Therefore, just as with equi-atomic alloys, thermomechanical processing has been mostly employed for modification of phase transformation. It is generally achieved by cold working and subsequent heat treatment (Ref 8). However, poor workability is an obstacle during cold working of NiTi alloys (Ref 9). In the literatures, most of the published studies have been focused on development of innovative techniques to modify phase transformation in Ni-rich and equi-atomic alloys, while little attention has been paid to Ti-rich alloys. As an appropriate candidate for high-temperature shape memory applications, it is worth studying new approaches to modify phase transformation in Ti-rich alloys. In this study, we investigate the effect of stress-assisted heat treatment on the microstructure and phase transformation of a Ti-rich alloy.

2. Experimental

An as-received rod of Ti-rich alloy with composition of Ti-49.52 at.% Ni provided by Special Metals Co. was used as the starting material. The rod then was annealed at temperature of 900 °C for 1 h in vacuum furnace followed by water quenching to room temperature (RT). The transformation temperatures of the annealed material were $M_s = 79.72$ °C, $M_f = 60.08$ °C, $A_s = 95.86$ °C, and $A_f = 110.33$ °C. In order to investigate the effect of applied stress during heat treatment, a creep instrument was used. The creep samples were prepared

A. Ahadi and E. Rezaei, Department of Materials Science and Engineering, Sharif University of Technology, Azadi Avenue, Tehran, Iran. Contact e-mail: Ebad.rezaei@gmail.com.

according to B577M ASTM standard with gauge diameter of 9 mm. Following cycles of heat treatment were conducted:

- 1- Heat treating at 500 °C without applied stress for 10 h (500-0-10).
- 2- Applied stress of +100 MPa at 500 °C for 10 h (500-100-10).
- 3- Applied stress of +200 MPa at 500 °C for 0.75 h (500-200-0.75).

The samples were heated up to 500 °C in 80 min under a very small preload of about 1 MPa. After completion of the tests, the stress was removed, and the samples were cooled down to RT in the chamber of creep furnace. Buttons with thickness of 1 mm were electro-discharge machined (EDM) from the mid-height of the heat-treated rods. Smaller buttons with diameter of 3 mm were EDM cut, mechanically ground to a thickness of 80 μm, and jet-electropolished in a solution composed of 30 vol.% HNO₃ and 70 vol.% methanol at temperature of -10 °C and voltage of 20 kV. A steady flow of cold water was used during mechanical grinding to preclude any possible phase transformation. Figure 1 shows schematic of the regions where the samples were extracted. The objective of extracting samples from the center of the buttons was to assure that they are not affected by oxidation at the extremities of the heat-treated rods. Microstructural observations were monitored with a Philips CM 200 instrument operated at an acceleration voltage of 200 kV. Room temperature XRD measurements were conducted using a Philips XRD apparatus operated at 40 kV and 30 mA equipped with a Cu-K_α radiation. Buttons with diameter of 3 mm and weight of 15 mg were thermal cycled up to 100 cycles with a TA Q-100 instrument with heating/cooling rates of 10 °C/min. After EDM cutting, surfaces of the samples were gently removed using a grit paper of 2500 to eliminate the effect of EDM cutting.

3. Results and Discussion

3.1 Microstructural Observation

In Fig. 2, the TEM microstructure of the material annealed at temperature of 900 °C for 1 h shows a relatively large Ti₂Ni precipitate together with regions of residual austenite (white

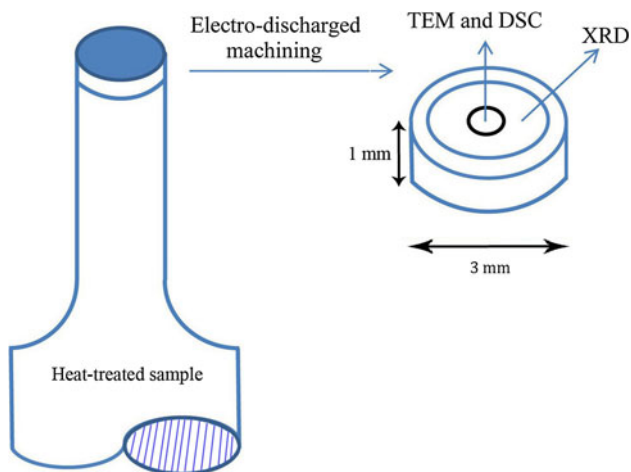


Fig. 1 A schematic of the regions studied for XRD, TEM, and DSC

areas) near the precipitate. The presence of residual austenite needs to be clarified, since at RT the material is below M_f and that a fully martensitic structure is expected. In NiTi alloys, due to severe affinity of Ti for oxidation, the Ti concentration of the layers near the oxidized surface decreases leading to a Ni-rich layer that decreases transformation temperatures drastically to below RT (Ref 10). Therefore, near the regions affected by oxidation, there is austenite phase at RT. It should be mentioned that the TEM thin foils were extracted from the center of the heat-treated rods, far enough from the extremities, so that they are not possibly affected by oxidation. The oxidation caused by EDM cutting was also removed as described in the experimental section. Thus, oxidation seems not to be the reason for the observation of residual austenite at RT. The presence of

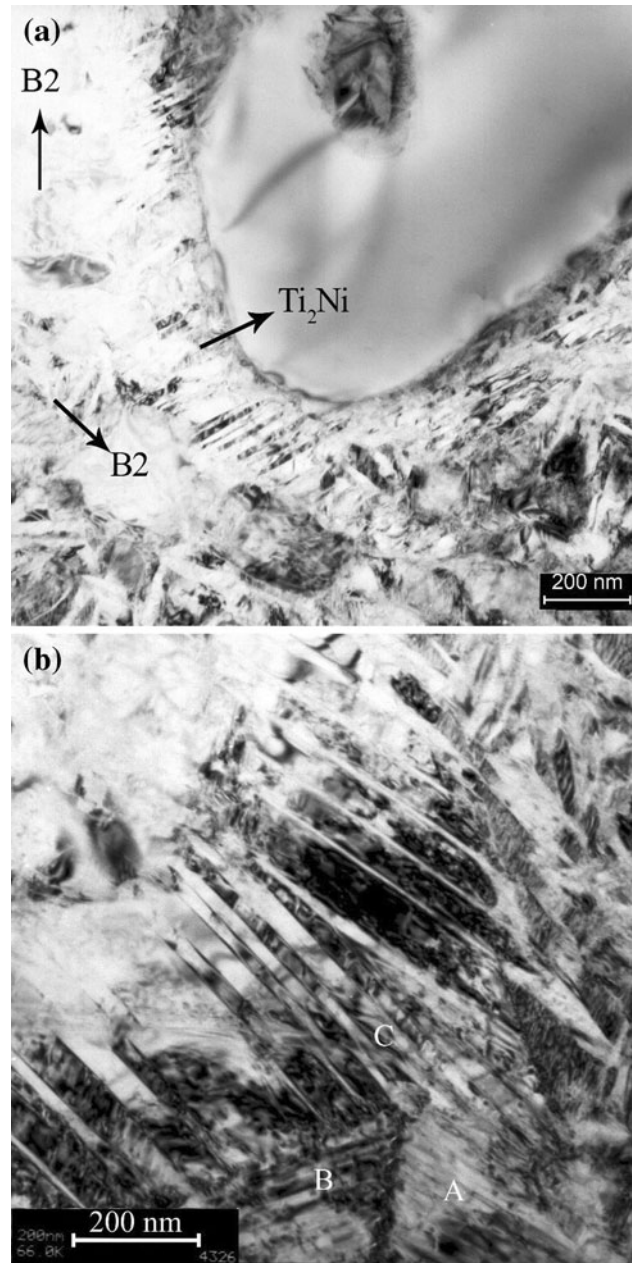


Fig. 2 TEM microstructure of the material annealed at 900 °C for 1 h. (a) Demonstrating a large Ti₂Ni precipitate and regions of residual austenite near the precipitate (b) Martensite plates (A, B, and C) showing a self-accommodating morphology

residual austenite can be attributed to local inhomogeneity in chemical composition as well as Ni-enrichment near the Ti_2Ni precipitate (Ref 11). Moreover, in Fig. 2(a) a dark hallow area within the Ti_2Ni precipitate is presumably indicative of some precipitate dissolution. Ti_2Ni precipitates eutectoidally decompose to $TiNi$ at temperature of 984 °C (Ref 7), therefore, some partial dissolution at temperature of 900 °C seems to be reasonable. Figure 2(b) illustrates a self-accommodating morphology of the martensite plates demonstrating all the characteristics of an undeformed microstructure in NiTi alloys, i.e. the interface between two martensite plates is straight and a strain contrast exists along the junction plane area (Ref 12). In Fig. 3 the microstructures of the 500-0-10 material shows the same features for the morphology of martensite similar to those observed in the annealed material. However, martensite plates have higher length in 500-0-10 material and residual austenite is not considerably present in the microstructure. Bringing in

mind that the annealed material has been water-quenched from 900 °C and the 500-0-10 material was slowly cooled in the chamber of creep furnace, these differences may be attributed to the different thermal stresses resulting from different cooling rates. By comparing Fig. 3(b) with morphology of martensite in other TEM studies (Ref 13), (100) compound twinning of the martensite is noticed in the 500-0-10 material. This type of martensite is a deformation twin and has been frequently observed near the edge of polishing hole in TEM samples (Ref 13). However, it is not clear that why this type of martensite was not observed in the annealed sample. Figure 4 demonstrates the diffractogram of the 500-0-10, 500-100-10, and 500-200-0.75 materials. From this figure one can notice the presence of different $B19'$ martensite reflections in the stress-free heat-treated material in conjunction with an almost weak reflection of austenite, implying a dominant martensitic microstructure. Although martensitic structure was expected (it will be described in “Phase Transformation” section where transformation temperatures are slightly shifted as a result of stress-assisted heat treatment), both stress-assisted heat-treated materials have a high intensity of austenite, indicating austenite phase as the main constituent of the microstructure. This is further confirmed by the TEM microstructure of the 500-100-10 material, Fig. 5(a) and (b), in which the microstructure mainly consists of austenite phase (bright regions). The XRD and TEM results provide enough evidence to claim the occurrence of austenite stabilization during stress-assisted heat treatment. Moreover, in Fig. 5(a) and (b), a high density of thin and long mechanical twins are also obvious in the microstructure. It is worth noting that mechanical twins were uniformly observed within the TEM thin foil. In Fig. 6, the TEM microstructure of the 500-200-0.75 material reveals thicker mechanical twins in conjunction with a relatively high density of structural defects at the interface of the twin plates. Furthermore, the interface of the twins is not straight. The observation of mechanical twins suggests that the austenite phase has experienced deformation during heat treatment and twinning is possibly an active mechanism of deformation. As such, the following discussion is crucial for interpretation of the results:

In general, the high temperature mechanism of deformation in NiTi shape memory alloys with B2 structure is dependent on the temperature. Since at low temperatures dislocation, motion

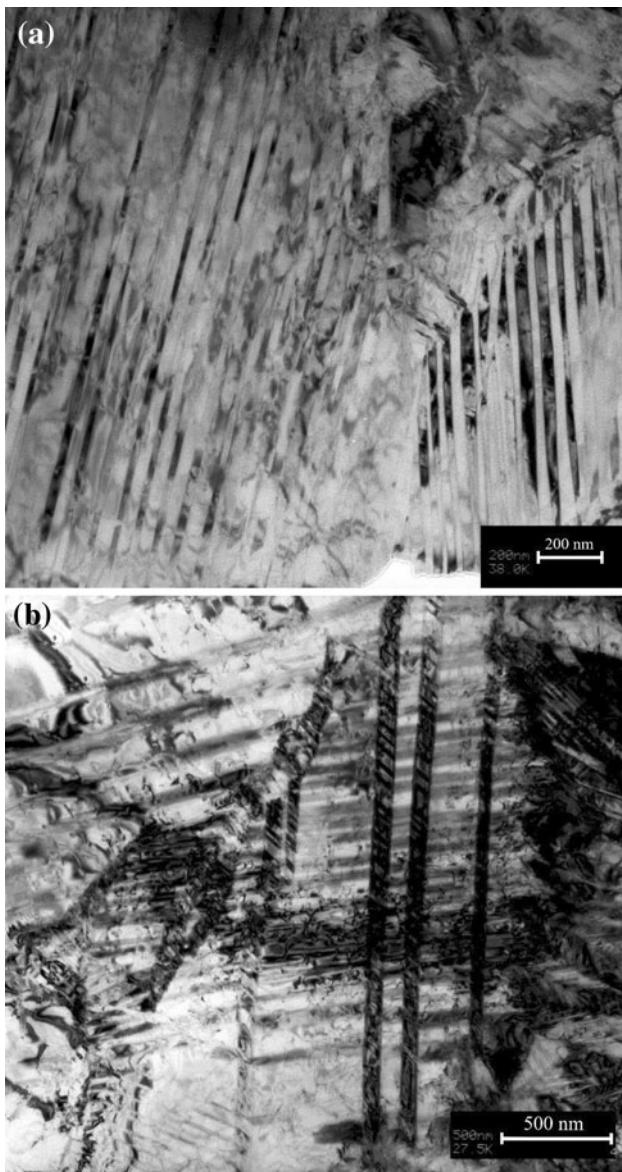


Fig. 3 TEM microstructure of the 500-0-10 material. (a) Self-accommodating morphology of the martensite and long martensite plates and (b) (100) compound twinning

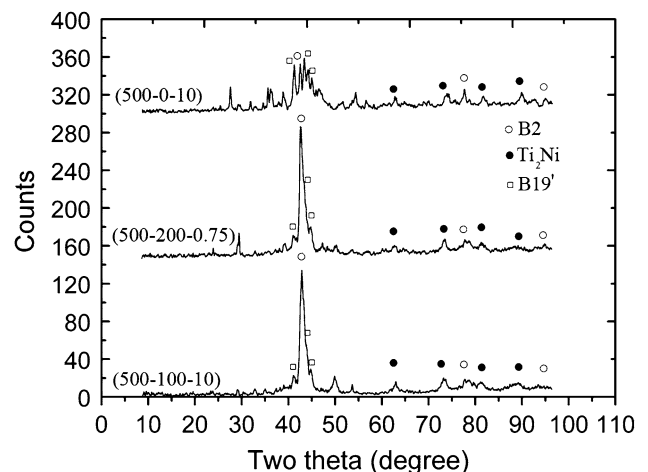


Fig. 4 XRD diffractograms of the heat-treated materials

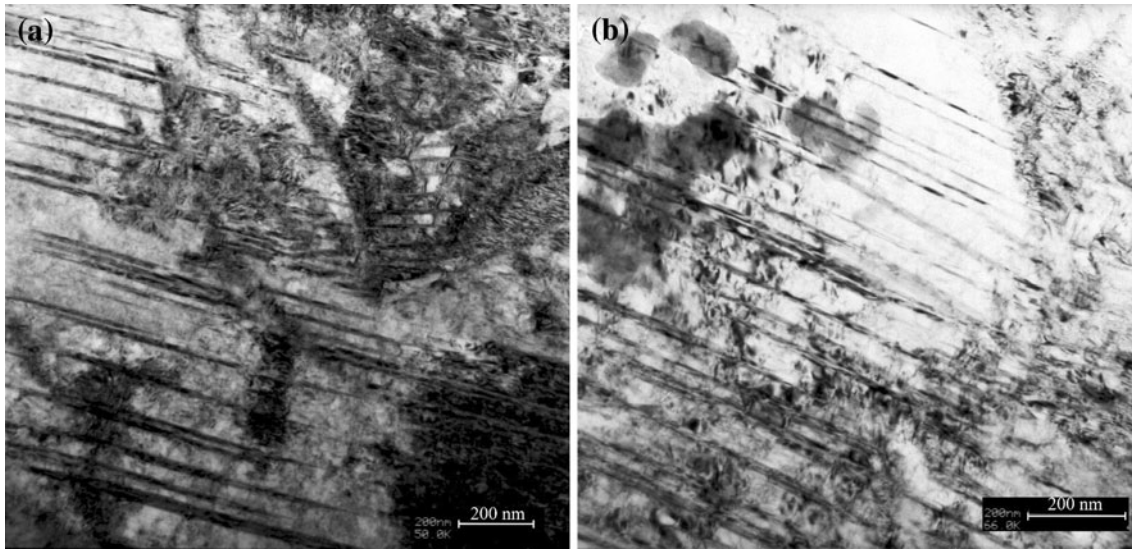


Fig. 5 TEM microstructure of the 500-100-10 material (a) showing mechanical twins stretched in austenitic matrix and (b) a different region in the TEM thin foil

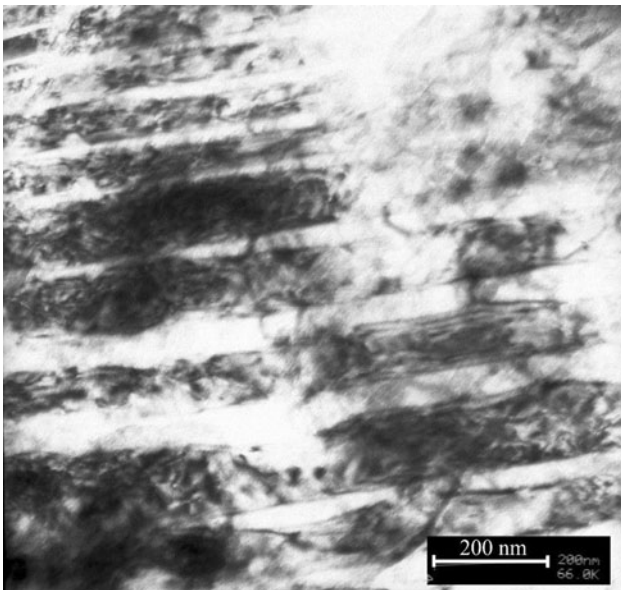


Fig. 6 TEM microstructure of 500-200-0.75 material. Notice that mechanical twins become larger

is not easy, the NiTi alloys deform via mechanical twinning which provides new slip systems (Ref 14). By increasing the deformation temperature, more slip systems become active and slip is the dominant mode of deformation. About the occurrence of mechanical twinning three aspects must be taken into account:

1. The extreme temperature at which deformation mechanism is changed.
2. The degree of deformation and its influence on degree of mechanical twinning.
3. Rate of deformation.

To the knowledge of the authors, there is no consensus about the extreme temperature. Hornbogen et al. reported the

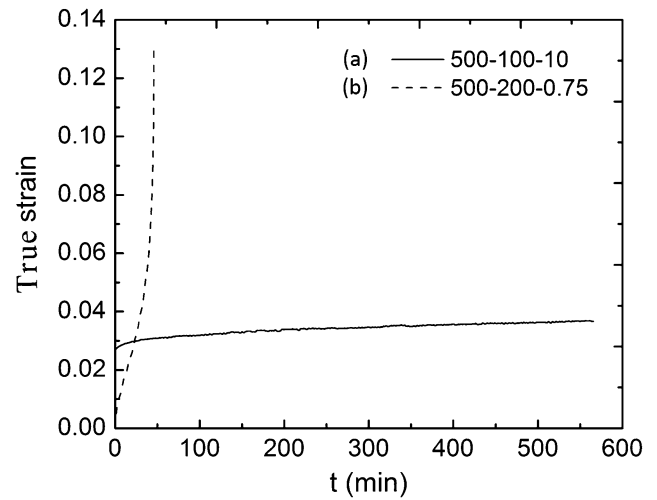


Fig. 7 Creep curves for (a) 500-100-10 and (b) 500-200-0.75 samples

temperature of 700 °C as the extreme temperature above which dislocation slip is the deformation mechanism, while, below 700 °C, a combination of mechanical twinning and dislocation slip are active (Ref 15). Formation of long mechanical twins has been also reported during warm severe plastic deformation at 450 °C (Ref 16) and warm rolling at temperature of 500 °C (Ref 17). From the perspective of temperature, the observation of mechanical twins during stress-assisted heat treatment at temperature of 500 °C is consistent with previous researches. However, this observation is peculiar with respect to the degree of deformation imposed to NiTi. In previous studies in which mechanical twins have been observed during warm deformation, (Ref 15-17), a high degree of deformation such as 20 and 50% elongation have been imposed to the NiTi while in this study, the deformation is small. To show the degree of deformation in the stress-assisted heat-treated materials the creep curves are shown in Fig. 7. The curves show significant differences in terms of the creep stage as well as the degree of

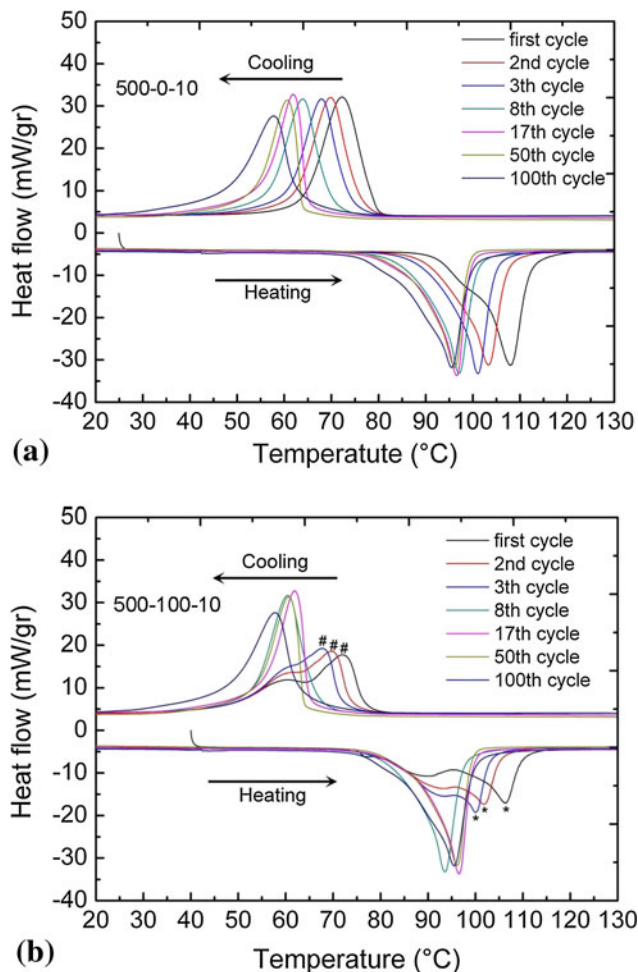


Fig. 8 DSC thermograms during thermal cycling for (a) 500-0-10 and (b) 500-100-10 material

creep strain. While the 500-100-10 material is in the primary creep stage (first stage of the creep) with small tensile strain of 0.03, the 500-200-0.75 material is in the tertiary creep stage (third stage of the creep) and has experienced a tensile strain of about 0.13. Thus, we report the presence of a high density of mechanical twins at very small tensile strain of about 0.03 which has not been reported before. Tensile deformation is likely to be responsible for the observation of high density of mechanical twins at such a small strain. In the deformation processes used in (Ref 15-17) (Rolling, swaging, and Equal-channel angular pressing), due to the complex stress state more slip systems are possibly activated and slip tends to be the dominant mode of deformation. While, in tensile deformation, a limited number of slip systems are activated and mechanical twinning is more necessitated even at small strains to accommodate deformation. The degree of deformation is also an influential parameter on the density of mechanical twins. The larger the degree of deformation, the higher the density of twins (Ref 18). The increase in size of twins resulting from increasing applied stress during heat treatment, as was noted by comparing Fig. 5 and Fig. 6, is in accordance with previous studies. Rate of deformation is also important as deformation heating is significant in NiTi shape memory alloys (Ref 19). The temperature increase during deformation, if considerable, can cause slip to become active as a deformation mechanism.

However, the rate of deformation during creep is slow and cannot cause deformation heating.

The results reported here on the observation of a high density of mechanical twins at very small tensile strain and low rates of deformation is of great importance. However; the detailed mechanisms supporting this phenomenon is not clear and yet to be explained.

3.2 Phase transformation

In Fig. 8(a) and (b) the evolution of transformation during repeated thermal cycling of 500-0-10 and 500-100-10 materials are shown, respectively. It is worth noting that the term "thermal cycling," refers to cycling tests in the differential scanning calorimeter and should not be misunderstood by thermo-mechanical cycling. Obviously, stress-assisted heat treatment does not suppress martensitic transformation, and the change in transformation temperatures is not considerable, see Fig. 8(a). A single-stage transformation during forward tends to a small two-stage transformation in the cycles of reverse transformation in the 500-0-10 material. In the 500-100-10 material, the two-stage transformations are more conspicuous during both heating and cooling cycles. On further increasing the number of thermal cycles, the transformation temperatures decrease with almost the same rate for both materials, and the two-stage transformation gradually diminishes. A single-stage transformation evolves after about eight cycles of transformation. The decrease in transformation temperatures during thermal cycling is well-documented (Ref 20) and is not discussed here for the purpose of brevity. However, the observation of two-stage transformation and its disappearance after thermal cycling is of great importance since it has been observed by Liu et al. (Ref 21) and Paula et al. (Ref 22) for Ti-rich alloys, but has not been discussed.

Often two or multi-stage transformation is attributed to the intermediate (R-phase) or inhomogeneous transformation. The observed two-stage transformation in the 500-100-10 material is not attributed to R-phase transformation, inasmuch as it is not developing or stabilizing during thermal cycling (Ref 20). The inhomogeneous transformation has been observed in Ni-rich alloys (Ref 23) as well as in alloys where there has been an unequal distribution of grain size (Ref 24). The latter case has been reported in intensively cold-rolled and annealed NiTi and is not likely to be responsible for the observed two-stage transformation in 500-100-10 material. In Ni-rich alloys, fine Ti_3Ni_4 precipitates account for multi-stage transformation, while, in the case of Ti-rich alloys, it is not clear if the stress field around Ti_2Ni precipitates is able to promote local transformation. In Ti-rich alloys the elastic moduli mismatches between Ti_2Ni /matrix interface is the main reason for development of interfacial stresses (Ref 25). In addition, externally induced stresses can also cause significant stress concentration at Ti_2Ni /matrix interface. The presence of stress field surrounding a precipitate can promote local transformation manifested by different peaks in DSC curves (Ref 4, 5). The local stress fields are well-manifested by dark regions around precipitates in TEM images (Ref 26). The interface of Ti_2Ni /matrix in the annealed sample, Fig. 1(a), was bright indicating insignificant stress field being likely due to the large size of the precipitate. However, when a stress is applied during heat treatment, a dark region around the Ti_2Ni precipitate appeared and deformation lines passed through the precipitate as is observed in Fig. 9(a) and (b). Therefore, it is suggested that the accommodation of

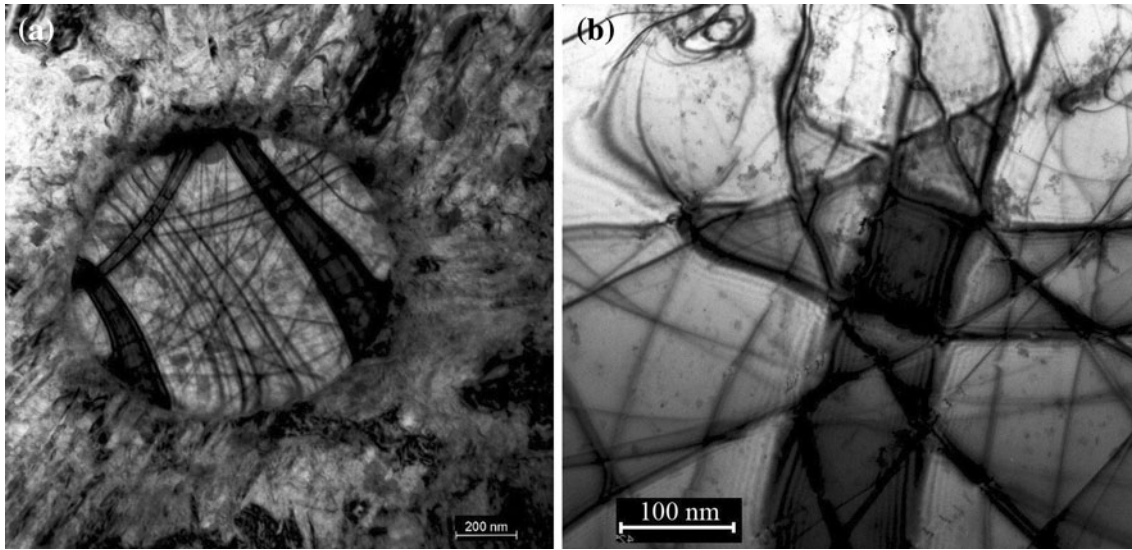


Fig. 9 TEM microstructure of the 500-100-10 material (a) showing the presence of stress field at Ti_2Ni /matrix interface and (b) enlarged region within the Ti_2Ni precipitate demonstrating the deformation lines pass through the precipitate

stresses at Ti_2Ni /matrix is effective in local modification of phase transformation which leads to two-stage transformation in the stress-assisted heat-treated material. For the 500-0-10 material, the elastic moduli mismatches between Ti_2Ni /matrix do not provide a strong stress field to assist local transformation.

The reason that transformation is affected by the presence of stress field surrounding a precipitate can be expressed by the following equation (Ref 26, 27):

$$M_s = T_0 + \frac{\Delta E_c^d}{\Delta S^{A-M}} \quad (\text{Eq 1})$$

where T_0 is the equilibrium temperature between the martensitic and the parent phase at which the Gibbs free energies of the two phases are equal, M_s is the martensitic start transformation temperature, ΔS^{A-M} is the entropy change, and $\Delta E_c^d = -\sigma_{ij}^t \epsilon_{ij}^t$ is the elastic strain energy introduced by the presence of a defect. The equation shows that the transformation temperature can be locally modified by the presence of a stress field surrounding a precipitate. The resulting shift will be proportional to the stress field and inversely to entropy. It is believed that the first peak in cooling (marked by # in Fig. 8a) belongs to local B2 to B19' transformation at Ti_2Ni /matrix interface and the second peak in heating (marked by * in Fig. 8b) belongs to the reverse B19' to B2 transformation at stressed regions around Ti_2Ni precipitate. This is a rule that the B2 to B19' transformation occurring at high temperatures has a reverse B19' to B2 transition at higher temperatures. Introduction of structural defects during thermal cycling counteract the stress field at Ti_2Ni /matrix interface giving rise to a single-stage transformation. It is worth noting that due to the complexity of the microstructure in the stress-assisted heat-treated materials, it was not possible to reveal the martensite plates nucleating at Ti_2Ni /matrix interface to propose compelling evidence as to the role of stress accommodation on modification of transformation. A further TEM work on the role of precipitates as nucleation sites is under way, and the results will be presented elsewhere.

4. Conclusions

In this study, the effect of stress applied during heat treatment of a Ti-rich NiTi shape memory alloy was investigated. The following are conclusions made in this study:

1. XRD and TEM results revealed that the RT microstructure of the stress-assisted heat-treated materials was partly composed of austenite. This microstructure was significantly different from the stress-free heat-treated material in which long variants of self-accommodating martensite were the prominent features of the microstructure.
2. A high density of mechanical twins was observed in the microstructure at very small tensile strain of 0.03 indicating twinning as an active mode of deformation. The size of mechanical twins was increased with increasing the value of applied stress.
3. Stress-assisted heat treatment caused a two-stage phase transformation in the initial cycles of transformation. With further thermal cycling up to 100 cycles the two-stage transformation was replaced by a single-stage transformation.
4. It was proposed that the accommodation of stresses at Ti_2Ni /matrix interface brings about a thermodynamically suitable condition for nucleation of martensite variants which is manifested by a two-stage phase transformation. Introduction of structural defects during thermal cycling counteract the stress field causing a single-stage transformation after about eight cycles.

Acknowledgments

The authors would like to thank the Sharif University of Technology, Tehran, Iran for the financial support and provision of the research facilities used during this study. The authors also would like to thank Dr. W.J. Moberly Chan for his fruitful discussions in improving the content of this article.

References

1. T. Duerig, A. Pelton, and D. Stöckel, An Overview of Nitinol Medical Applications, *Mater. Sci. Eng. A.*, 1999, **273–275**, p 149–160
2. D.C. Lagoudas, *Shape Memory Alloys Modeling and Engineering Applications*, first ed., 2008, Springer, New York, p 30
3. T. Kurita, H. Matsumoto, and H. Abe, Transformation Behavior in Rolled NiTi, *J. Alloys Compd.*, 2004, **381**, p 158–161
4. J.I. Kim, Y. Liu, and S. Miyazaki, Ageing-Induced Two-Stage R-Phase Transformation in Ti-50.9at.%Ni, *Acta Mater.*, 2004, **52**, p 487–499
5. Y. Zheng, F. Jiang, L. Li, H. Yang, and Y. Liu, Effect of Ageing Treatment on the Transformation Behavior of Ti-50.9 at.% Ni Alloy, *Acta Mater.*, 2008, **56**, p 736–745
6. H.F. Lopez, A. Salinas-Rodriguez, and J.L. Rodriguez-Galicia, Microstructural Aspects of Precipitation and Martensitic Transformation in a Ti-Rich Ni-Ti Alloy, *Scr. Mater.*, 1996, **34**, p 659–664
7. K. Otsuka and X. Ren, Physical Metallurgy of Ti-Ni-Based Shape Memory Alloys, *Prog. Mater. Sci.*, 2005, **50**, p 511–678
8. A.S. Paula, K.K. Mahesh, C.M.L. dos Santos, F.M. Braz Fernandes, and C.S. da Costa Viana, Thermomechanical Behavior of Ti-Rich NiTi Shape Memory Alloys, *Mater. Sci. Eng. A*, 2008, **481–482**, p 146–150
9. M.H. Wu, Fabrication of Nitinol Materials and Components, *Mater. Sci. Forum*, 2002, **394–395**, p 285–292
10. K.S. Kim, K.K. Jee, W.C. Kim, W.Y. Jang, and S.H. Han, Effect of Heat Treatment Temperature on Oxidation Behavior in Ni-Ti Alloy, *Mater. Sci. Eng. A*, 2008, **481–482**, p 658–661
11. B. Bertheville and J.-E. Bidaux, Alternative Powder Metallurgical Processing of Ti-Rich NiTi Shape-Memory Alloys, *Scr. Mater.*, 2005, **52**, p 507–512
12. Y. Liu, Z. Xie, J. Van Humbeeck, L. Delaey, and Y. Liu, On the Deformation of the Twinned Domain in NiTi Shape Memory Alloys, *Philos. Mag. A*, 2000, **80**, p 1935–1953
13. M. Nishida, H. Ohgi, I. Itai, A. Chiba, and K. Yamauchi, Electron Microscopy Studies of Twin Morphologies in B19' Martensite in the Ti-Ni Shape Memory Alloy, *Acta Metal. Mater.*, 1995, **43**, p 1219–1227
14. W.J. Moberly, T.W. Duerig, J.L. Proft, and R. Sinclair, Mechanical Twinning and Plasticity in Ti-Ni-Fe (3%), *Mater. Sci. Forum*, 1990, **56–58**, p 759–764
15. E. Hornbogen, Ausforming of NiTi, *J. Mater. Sci.*, 1999, **34**, p 599–606
16. A.V. Kulkarni, Effect of Ausforming via Severe Plastic Deformation on Shape Memory Behavior of NiTi, M.Sc. Thesis, 2004, Texas A&M University, p 42
17. W.J. Moberly, Mechanical Twinning and Twinless Martensite in Ternary Ti_xNi(50–x)M_x, PhD Thesis, Stanford University, 1991, p 214
18. W.J. Moberly, Mechanical Twinning and Twinless Martensite in Ternary Ti_xNi(50–x)M_x, PhD Thesis, Stanford University, 1991, p 204
19. A. Ahadi, A. Karimi Taheri, K. Karimi Taheri, I.S. Sarraf, S.M. Abbasi, The Effect of Deformation Heating on Restoration and Constitutive Equation of a Wrought Equi-Atomic NiTi Alloy, *J. Mater. Eng. Perform.*, 2011. doi:10.1007/s11665-011-9936-x
20. J. Uchil, K. Ganesh Kumara, and K.K. Mahesh, Effect of Thermal Cycling on R-Phase Stability in a NiTi Shape Memory Alloy, *Mater. Sci. Eng. A*, 2002, **332**, p 25–28
21. Y. Liu, M. Blanc, G. Tan, J.I. Kim, and S. Miyazaki, Effect of Ageing on the Transformation Behaviour of Ti-49.5 at.% Ni, *Mater. Sci. Eng. A*, 2006, **438–440**, p 617–621
22. A.S. Paula, J.P.H.G. Canejo, R.M.S. Martins, and F.M. Braz Fernandes, Effect of Thermal Cycling on the Transformation Temperature Ranges of a Ni-Ti Shape Memory Alloy, *Mater. Sci. Eng. A*, 2004, **378**, p 92–96
23. G. Fan, Y. Zhou, W. Chen, S. Yang, X. Ren, and K. Otsuka, Precipitation Kinetics of Ti₃Ni₄ in Polycrystalline Ni-Rich TiNi Alloys and Its Relation to Abnormal Multi-Stage Transformation Behavior, *Mater. Sci. Eng. A*, 2006, **438–440**, p 622–626
24. S.H. Chang, S.K. Wu, and G.H. Chang, Grain Size Effect on Multiple-Stage Transformations of a Cold-Rolled and Annealed Equiatomic TiNi Alloy, *Scr. Mater.*, 2005, **52**, p 1341–1346
25. H.F. Lopez, A. Salinas, and H. Calderon, Plastic Straining Effects on the Microstructure of a Ti-Rich NiTi Shape Memory Alloy, *Met. Metall. Mater. Trans. A*, 2001, **32A**, p 717–729
26. E. Bataillard, J.-E. Bidaux, and R. Gotthardt, Interaction Between Microstructure and Multiple-Step Transformation in Binary NiTi Alloys Using In-Situ Transmission Electron Microscopy Observations, *Phil. Mag.*, 1998, **78**, p 327–344
27. X.T. Zu, L.B. Lin, Z.G. Wang, S. Zhu, L.P. You, L.M. Wang, and Y. Huo, Influence of Electron Irradiation on the Martensitic Transformation of a Binary TiNi Shape Memory Alloy, *J. Alloys Compd.*, 2003, **351**, p 87–90